



FATIGUE CRACK INITIATION AND PROPAGATION OF A TiNi SHAPE MEMORY ALLOY

Anne-Lise Gloanec, Priscillia Cerrachio, Bertrand Reynier, Alain van Herpen,
Patrice Riberty

► To cite this version:

Anne-Lise Gloanec, Priscillia Cerrachio, Bertrand Reynier, Alain van Herpen, Patrice Riberty. FATIGUE CRACK INITIATION AND PROPAGATION OF A TiNi SHAPE MEMORY ALLOY. Scripta Materialia, 2010, volume 62, pp.786-789. 10.1016/j.scriptamat.2010.02.001 . hal-00660662

HAL Id: hal-00660662

<https://ensta-paris.hal.science/hal-00660662>

Submitted on 19 Jan 2012

HAL is a multi-disciplinary open access archive for the deposit and dissemination of scientific research documents, whether they are published or not. The documents may come from teaching and research institutions in France or abroad, or from public or private research centers.

L'archive ouverte pluridisciplinaire **HAL**, est destinée au dépôt et à la diffusion de documents scientifiques de niveau recherche, publiés ou non, émanant des établissements d'enseignement et de recherche français ou étrangers, des laboratoires publics ou privés.

FATIGUE CRACK INITIATION AND PROPAGATION OF A TiNi SHAPE MEMORY ALLOY

A.-L. Gloanec, P. Cerracchio, B. Reynier, A. Van Herpen, P. Riberty
UME/MS-ENSTA Paristech, 32 boulevard Victor, 75732 Paris Cedex 15, France

Abstract

In this paper, fatigue crack initiation and propagation stages of a TiNi shape memory alloy are examined thanks to a low cycle fatigue interrupted test. Submitted to fatigue cyclic loading, the response of the alloy presents a classical pseudoelastic response. Two potential initiation crack areas are highlighted: at the phase interfaces or at the grain boundaries. Then, propagation results from the coalescence of many microscopic cracks. These two stages are detectable at the last 20% of the total fatigue life.

Keywords

Low cycle fatigue; Pseudoelastic behavior; Fatigue crack initiation; Fatigue crack propagation; Dissipated energy.

Introduction

Shape memory alloys (SMA) are fascinating materials. Contrary to usual metallic alloys, they exhibit very specific thermo-mechanical behaviors : including shape memory effect [1, 2], two-way shape memory effect [2], superelasticity [3-5] and damping [6]. Many engineering applications have been developed using these properties in various fields (medical, aeronautic, automobile, domestic or civil engineering).

Within the frame of design and reliability of systems using SMA, it is essential to have phenomenological models representing as well as possible fatigue thermo-mechanical behavior. To do that, understanding physical mechanisms governing the cyclic behavior and leading to the degradation is a necessary step.

In this paper, one will focus on superelasticity, also called pseudoelasticity, which describes the capacity of the SMA to support very significant recoverable deformation when a mechanical effort is applied. This deformation results from an austenite-martensite transformation under isothermal conditions, at a temperature greater than the finish temperature of the reverse martensite-austenite transformation. The aim of this paper is to detect fatigue crack initiation and propagation stages, and to link observations with cyclic behavior.

Material and Experimental Procedure

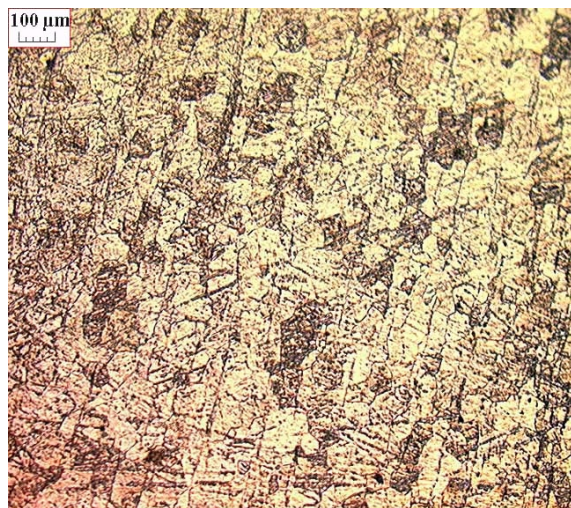
Material

The material investigated here is a near equiatomic TiNi alloy. More precisely, sample analyses showed that the composition is 51.3% (at.) Ti and 48.7% (at.) Ni.

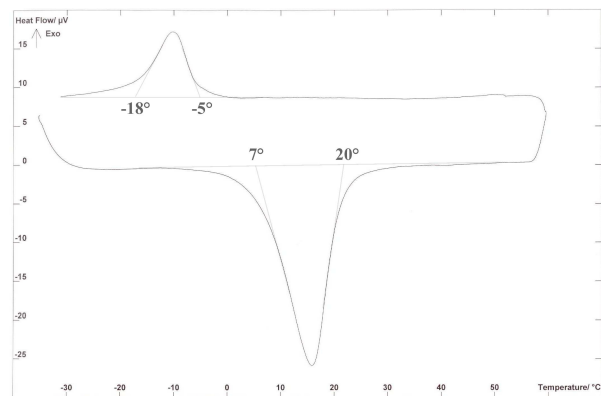
In order to develop pseudoelastic behavior, a particular thermo-mechanical treatment was carried out:

- a first *heat treatment* consisting in maintaining at 850°C during 1h followed by water quenching. At this temperature, above the recrystallization one in the austenitic field [7, 8], work hardening, due to machining, is thus eliminated.
- a *mechanical treatment* consisting in a work hardening from 0 to 550 MPa at 200°C. A high dislocation density is then introduced. This implies an increase of the resistance for slip deformation by raising the critical stress for slip [9-11].
- finally, a second *heat treatment* consisting in maintaining at 400°C during 1h. At this temperature, below the recrystallization one, the high dislocation density is maintained [11].

The resulting microstructure is mainly made of fine grains with an average size of 25 μm (Figure 1 a-).



a- Microstructure



b-DSC measurements

Figure 1 : Properties of NiTi alloy

The transformation temperatures can be obtained by Differential Scanning Calorimetry (DSC) measurements [12].

Figure 1 b- displays a DSC thermogram (heat flow versus temperature). Initially, the material specimen was heated from approximately - 40°C to 60°C (lower part of the curve). At low temperatures the material is in martensite phase. The heat flow peak at a temperature of approximately 16°C corresponds to an endothermic transition to an austenitic phase. The area under this peak represents the latent heat of transformation and the construction lines indicate the values of the start ($A_s = 7^\circ\text{C}$) and finish ($A_f = 20^\circ\text{C}$) temperatures of the transition. Then, the material was cooled from approximately 60°C to - 40°C (upper part of the curve). The heat flow peak at a temperature of approximately - 10°C corresponds to an exothermic transition to a martensite phase. The start temperature of the transition is $M_s = - 5^\circ\text{C}$ and the finish one is $M_f = - 18^\circ\text{C}$.

Test specimen

The test specimen used was cylindrical with a gauge section of 8 mm in diameter and 20 mm in length and a total length of 120 mm. A mechanical polishing of the gauge length was carried out with silicon carbon paper in order to minimize the effects of the surface irregularities, like work hardening due to machining or oxide layers developed at 850°C. The final surface preparation was then achieved by an electrolytic polishing.

Fatigue Test

A low cycle fatigue test was conducted on a servo-hydraulic machine (MTS 810) controlled in force (from 0 to 23.4 kN) at 1 Hz. In order to work on austenitic phase, the test was performed at 50°C. The signal was sinusoidal in shape with a null stress ratio.

The strain amplitude was measured by an EPSILON extensometer with a root of 10 mm, placed on the gauge of the test specimen.

The aim was to observe the initiation of cracks (size between 5 and 10 μm) and to follow the growth of the latter. The test was stopped at various stages of cycling and disconnected from the servo-hydraulic machine. At each stop, observations of the specimen surface were carried out in a JEOL Scanning Electron Microscope (JSM 5910 LV). The observations reported here were noticed in a homogeneous way on the test specimen surface.

Results and Discussion

In this paper, results about cyclic behavior will be presented in two shapes :

- first one : hysteresis loops (Figure 2 a - and Figure 2 b -), which describe stress-strain behavior,
- second one : dissipated energy versus number of cycles (Figure 2 c -), the dissipated energy being equal to the surface of the hysteresis loop in the strain-stress curve.

During its fatigue life, the material investigated here, presents two different behaviors:

- Firstly, from cycle 1 to 1259 one (Figure 2 a-), a classical pseudoelastic response may be observed. Although the test is stopped, the cyclic behavior looks like the one described by Moumni et al. [4] or by Miyazaki et al. [11] on not stopped tests. Namely the strain-stress response is characterized by hysteresis loops which evolve during cycling. Indeed they change their form and become smaller. Nevertheless, this change tends to stabilize with increasing the number of cycles. As many authors [6, 11, 13, 14] this stabilization effect occurs around the 100th cycle. Contrary to Moumni et al. [4] or Paradis et al. [13], no residual strain is noticed after the first unloading. Residual strain starts to appear at the end of the second unloading, increases during cycling and tends to saturate with a value of 0.4%. Note that in order to observe the surface of the specimen, the test is stopped and the specimen is disconnected from the machine. But after this pause, at the resumption of cycling, the form of the hysteresis loop remain unchanged. This behavior, reported in a diagram giving the dissipated energy versus the number of cycles (Figure 2 c -), shows a rapid decrease during the ten first cycles followed by a slight decrease until around the 100th cycle and a complete stabilization until cycle 1250.

- Secondly, from cycle 1260 to fracture, the TiNi alloy still presents a classical pseudoelastic response (Figure 2 b-), but now, cycling interruptions significantly impact the shape of the hysteresis loops and so the dissipated energy (Figure 2 c-). Immediately after a pause (cycle 1260, 1310 or 1360) there is a discontinuity : the value of the dissipated energy increases after each stop in the cyclic loading. However, the global variation of the dissipated

energy remains unchanged if cycling allows it: a rapidly decrease then a stabilization, (Figure 2 c-).

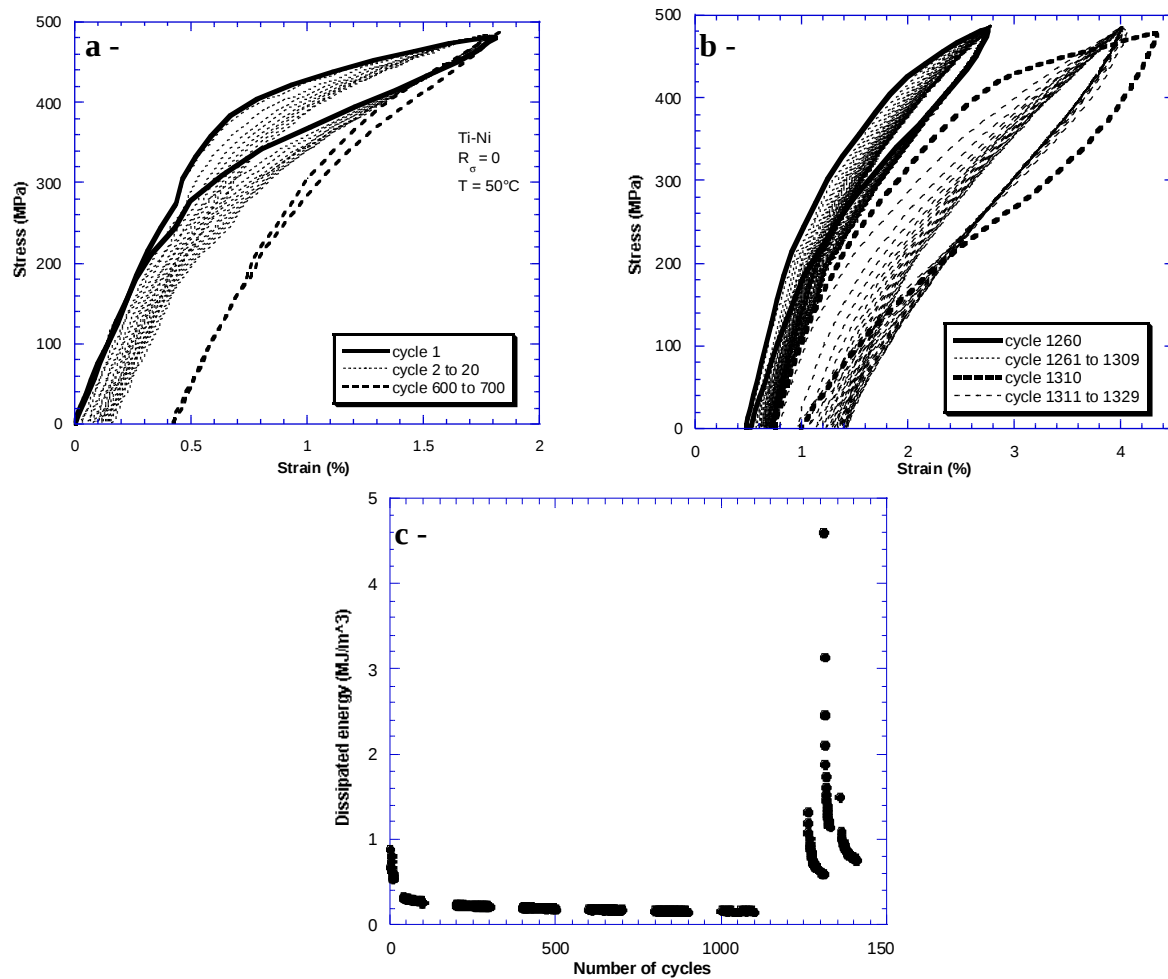


Figure 2 : Cyclic behavior (a- pseudoelastic behavior, cycle 1 to 1250 ; b- pseudoelastic behavior, cycle 1260 to 1329 ; c- dissipated energy versus number of cycles)

Many authors [5, 13, 15] reported the same kind of behavior for TiNi. For them, carrying out pauses between sets of cycles imply a dissipation of energy after each resumption of cycling. When cyclic loading is paused, a phenomenon called “strain recovery” occurs. Paradis et al. [5] explained that the residual strain, believed to be irreversible, can be partially recovered. In this study, an increase of the dissipated energy after a pause in cycling is just observed after the 1260th cycle and not as soon as the cyclic loading is stopped contrary to authors previously quoted [5, 13, 15]. The phenomenon of “strain recovery” could not be highlighted in this study. Indeed, for each SEM observation, the test specimen was disconnected from the servo-hydraulic machine, concealing thus “strain recovery”. Here the increase of the dissipated energy observed after a pause could be due to damage, namely crack initiation and growth. Various SEM observations of the specimen were performed at various stages, in order to detect crack initiation and to follow crack growth. Until cycle 1260 no crack was observed, only the formation of line traces in the grains (Figure 3 a-). These line traces indicate the stress-induced martensite plates. As reported by Miyazaki et al. [11], these residual martensite plates increase with the number of cycles and are considered to be one of the cause for the residual strain formed during cyclic loading. The present observations confirm this statement : higher the number of cycles is, more martensite plates appear.

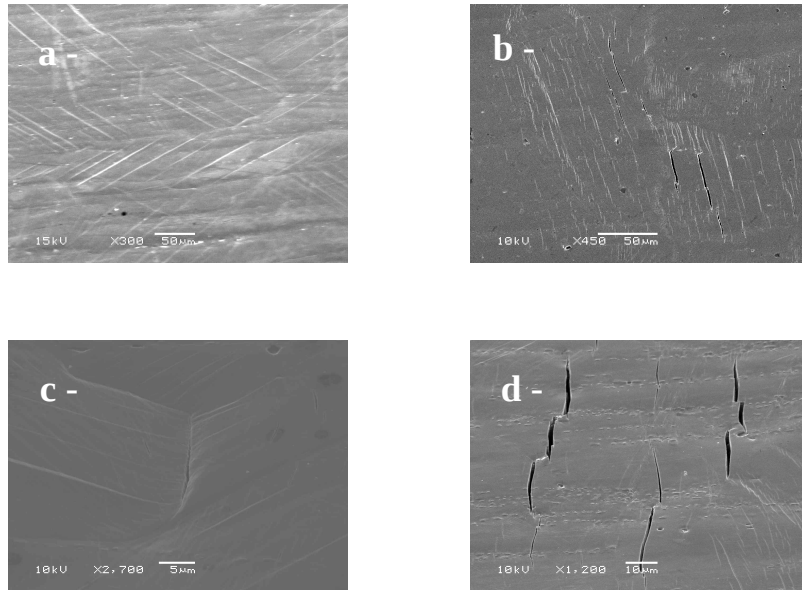


Figure 3 : SEM observations of the test specimen surface (a- martensite plates, b- crack initiation at martensite-martensite interfaces, c- crack initiation at grain boundaries, d- crack propagation)

In this study, for this material, two crack initiation areas could be distinguished:

- at the martensite-martensite or austenite-martensite interfaces (Figure 3 b-) as already mentioned by Miyazaki et al. [11]. For these authors, martensite-martensite or austenite-martensite interfaces motion cause the formation of defects in the grain, these defects becoming potential crack initiation areas.

- at grain boundaries (Figure 3 c-). This observation is in contradiction with the results of Melton and Mercier [16], for which, TiNi memory shape alloy does not exhibit a brittleness with grain boundaries.

Nevertheless, phase interfaces seem to be the preferential areas for crack initiation. Here, more cracks have been observed in the grains than at the grain boundaries.

After the first crack initiation observed (cycle 1260), during a set of cycles, the number of micro-cracks increases much more quickly than the size of these micro-cracks. In steels for Hornbogen [17], during cycling the martensite transformation kept the crack growth off. Indeed, this transformation could induce an internal compressive stresses ahead of the crack tip thus delaying its growth. The same phenomenon could take place in TiNi. The martensite transformation blocks the crack propagation to the detriment of microscopic cracks nucleation. It is only about the 1400th cycle that all microscopic cracks join together, causing the rapid growth of the crack size (Figure 3 d-).

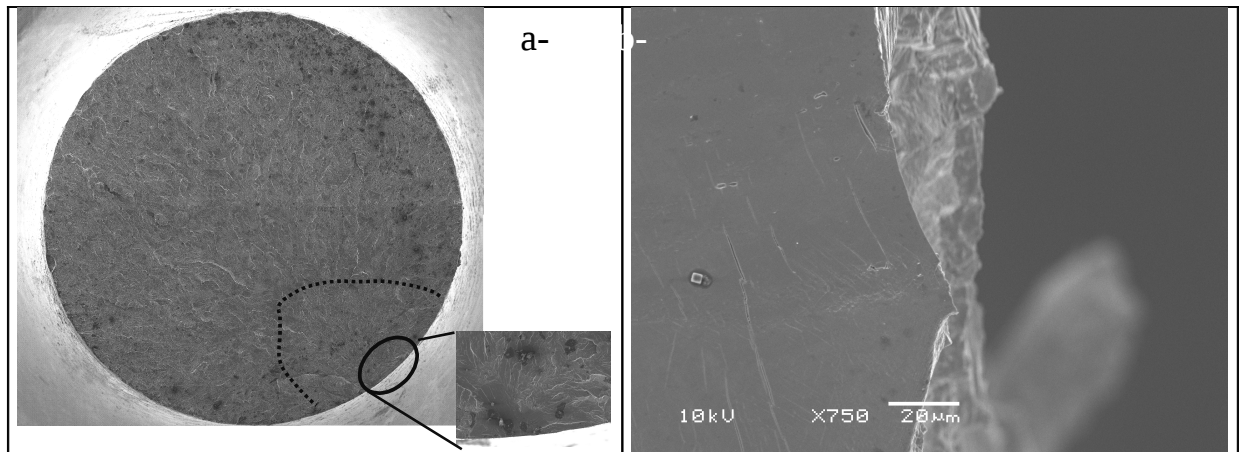


Figure 4 : Observations of the fracture surface

The fracture surface presents a brittle feature, namely a smoother fracture surface without secondary cracks. Regarding more closely, the initiation site (full line on Figure 4 a-), the propagation stage (dotted line on Figure 4 a-) and the final fracture are clearly identifiable. While observing the specimen surface at the initiation place, note that initiation is the result of the coalescence of several microscopic cracks (Figure 4 b-). The specimen broke at the cycle 1576, that means the visible damage, namely initiation and the propagation stages, represents the last 20 % of the fatigue life.

Conclusion

Fatigue crack initiation and propagation have been investigated on a TiNi shape memory alloy thanks to a low cycle fatigue interrupted test. In order to observe the initiation of cracks and to follow the growth of the latter, many observations of the test specimen were carried out between sets of cycles. The following conclusions can be established:

1. During its fatigue life the TiNi investigated here presents a classical pseudoelastic behavior. Namely the strain-stress response is characterized by hysteresis loops which evolve during cycling. Indeed they change their form and become smaller. Nevertheless, this change tends to stabilize with increasing the number of cycles.
2. If the strain-stress response is reported in a diagram giving the dissipated energy versus the number of cycles, the evolution of the dissipated energy presents two different behaviors :
 - firstly, from cycle 1 to 1259 one, a rapid decrease during ten first cycles followed by a slight decrease until around the 100th cycle and a complete stabilization until cycle 1250. No discontinuity was observed although the test was stopped.
 - secondly, from cycle 1260 to fracture, many discontinuities were noticed. Indeed an increase of the dissipated energy is observed after each resumption of cycling.
3. Because of the test procedure, no “strain recovery” has been clearly highlighted in this study. Nevertheless, SEM observations reveal that the increase of the dissipated energy may be linked to microscopic crack initiation. Two sites of initiation have been reported : the first one, at the martensite-martensite or austenite-martensite interfaces and the second one at the grain boundaries.

Note that a complementary test will be soon carried out. This time, the observations of the specimen surface will be realized with a numerical microscope, without disconnected the specimen and the servo-hydraulic machine.

4. The visible damage, namely initiation and propagation stages, represents only the last 20 % of the total fatigue life of the specimen of TiNi.

References

- [1] H.A.Mohamed and J.Washburn, Metallurgical Transaction, 10 (1976) 7.
- [2] K.Otsuka and X.Ren, Intermetallics, 511-528 (1999) 7.
- [3] S.Nemat-Nasser and W.G.Guo, Shape Memory alloys Mechanics of Materials, 463-474 (2006) 38.
- [4] Z.Moumni, A.VanHerpen and P.Riberty, Smart Materials and Structures, S287-S292 (2005) 14.
- [5] A.Paradis, P.Terriault and V.Brailovski, Computational Materials Science, (2009) article in press.
- [6] M.C.Piedboeuf, R.Gauvin and M.Thomas, Journal of sound and vibration, 885-901 (1998) 214.
- [7] G.F.Bastin and G.D.Rieck, Metallurgical Transaction, 1817 (1974) 5.
- [8] T.Saburi, S.Nenno, Y.Nishimoto and M.Zeniya, Journal of Iron and Steel, 571 (1986) 72.
- [9] H.Sehitoglu, C.Efstathiou, H.J.Maier and Y.Chumlyakov, Mechanics of materials, 538-550 (2006) 38.
- [10] S.Miyazaki, Y.Ohmi, K.Otsuka and Y.Suzuki, International conference on martensite transformation, Belgium, Supplement to Journal of physique, C4-255 (1982) 43.
- [11] S.Miyazaki, T.Imai, Y.Igo and K.Otsuka, Metallurgical Transaction A, 115-120 (1986) 17A.
- [12] A.J.Shaw and S.Kyriakides, Journal of the Mechanics and Physics of Solids, 1243-1281 (1995) 43.
- [13] A.Paradis, P.Terriault, V.Brailovski and V.Torra, Smart materials and structures, 065027 (2008) 17.
- [14] M.Dolce and D.Cardone, International Journal of mechanical sciences, 2657-2677 (2001) 43.
- [15] V.Torra, A.Isalgue, F.Martorell, F.Casciati, F.C.Lovey, M.Peigney, P.Terriault, D.Tirelli and B.Zapico, PROTECT2009, Hayama, Japan, 2009
- [16] K.N.Melton and O.Mercier, Acta Metallurgica, 137-144 (1979) 27.
- [17] E.Hornbogen, Acta Metallurgica, 147-152 (1978) 26.